Sublimation and Infrared Spectral Properties of Ammonium Cyanide

Short title: Sublimation and IR Properties of Ammonium Cyanide

by

Perry A. Gerakines *[1], Yukiko Y. Yarnall [1,2], and Reggie L. Hudson [1]

[1] Astrochemistry Laboratory, NASA Goddard Space Flight Center, Greenbelt, MD 20771 USA

[2] Center for Space Science and Technology, University of Maryland, Baltimore County, Baltimore, Maryland, USA

* Corresponding author:

Perry A. Gerakines
Astrochemistry Laboratory (Code 691)
NASA Goddard Space Flight Center
Greenbelt, MD 20771 USA
perry.a.gerakines@nasa.gov
301-286-9179

Revised manuscript
Manuscript pages: 41 pages (includes figures and tables)
Tables: 3
Figures: 9

ABSTRACT

The ammonium ion (NH_4^+) has been suggested to be present in interstellar ices and has been observed on the surfaces of planetary bodies using infrared (IR) spectroscopy as the primary means of identification. Evidence for ammonium salts has also been found in the dust and surface ices of comet 67P/Churyumov-Gerasimenko. Here we present a laboratory study of ammonium cyanide (NH_4CN) and report on several properties of this compound, measured with higher accuracy than in previous reports, including its IR band strengths for use in quantifying its abundance in interstellar and planetary ices. We also report the first measurements since 1882 of NH_4CN vapor pressures, sublimation fluxes, and sublimation enthalpy measured at temperatures relevant to subliming cometary ices (134-155 K). The density and refractive index of NH_4CN at 125 K and the sublimation enthalpy and vapor pressures of NH_3 at ~100 K are also reported.

Keywords: Ices; IR spectroscopy; Comets; Infrared observations

1. INTRODUCTION

Ionic solids (i.e., salts) are readily formed by acid-base reactions and have been detected or are suspected to be present in planetary bodies. For example, salts are thought to be present on Ceres in the main asteroid belt (King et al., 1992; De Sanctis et al., 2020), on the surfaces of Pluto's satellites Nix and Hydra (Cook et al., 2018), and in the subsurface oceans of Jovian satellites such as Europa, which are expected to be briny (Zimmer et al., 2000).

Ammonium (NH_4^+) salts were detected, or their presence deduced, in the nucleus of comet 67P/Churyumov-Gerasimenko (67P) by measurements made by the instruments onboard the Rosetta spacecraft sent by the European Space Agency (ESA). The cometary dust in the vicinity of the nucleus contained a variety of ammonium salts as measured by the ROSINA instrument (Altwegg et al., 2020, 2022). Infrared (IR) reflection spectroscopy of the comet's surface using the VIRTIS instrument provided a tentative identification of the ammonium ion's absorption feature at a wavelength near 3.2 μm (Quirico et al., 2016; Poch et al., 2020, 2023), where the total surface abundance of ammonium was estimated to be as high as ~40% of the dust's total mass. Furthermore, the abundances of gases in the coma of 67P indicated that the dissociation of ammonium salts likely contributed to the observed abundances of ammonia (NH_3) and hydrogen cyanide (HCN). One possible contributor considered was ammonium cyanide (NH_4CN), although it was not detected directly, and its presence was inferred by the detection of other CN-bearing species by Altwegg et al. (2020). Altwegg et al. (2022) further analyzed ROSINA data and inferred that most of the NH_3 is likely in the form of ammonium salts in the dust grains, based on the similar total amounts of NH_3 and that of all detected acids. They further list HCN as the second-most abundant acid in the dust after H_2S, with implications for the relative abundance of NH_4CN as compared to other ammonium salts.

These results also imply that ammonium salts such as NH_4CN could be the parent source for NH_3 and HCN in the comae of many different comets and may be a

source of the missing N from cometary gas observations (Geiss, 1987). If ammonia was chemically altered and stored in a form that is more resistant to sublimation (such as NH_4CN or other ammonium salt), it might only be observed in a cometary coma at temperatures that drive the sublimation of the parent salt and its dissociation products. This hypothesis has led to some recent laboratory studies of ammonium-bearing salts and minerals, but usually for solids with a lower volatility than NH_4CN studied at room temperature (e.g. Hänni et al., 2019) and usually measured in reflectance (e.g., Fastelli et al., 2020).

Unidentified infrared features in the spectra of dense interstellar clouds suggest that NH_4^+ also may be present on interstellar grains. It has long been suggested that the absorption feature near 1400 cm^{-1} (~7 μm) is due to NH_4^+ (e.g., Grim et al., 1989; Schutte and Khanna, 2003; Boogert et al., 2015). Evidence in the IR spectra of interstellar ices does not support the presence of HCN or the CN^- anion, so the presence of NH_4CN in interstellar ice seems unlikely. However, one piece of circumstantial evidence in favor of the NH_4^+ cation as the carrier for the unidentified feature is that it could be the counter ion to a known anion in interstellar ices-specifically the cyanate anion OCN^- observed near 4.6 μm (Lacy et al., 1984). Other, as yet unidentified, counter ions also could be present, which seems likely given the cometary dust measurements from Rosetta described in the previous paragraphs.

Our recent work has focused on the IR spectra, physical properties (refractive indices and densities), band strengths, and optical constants of HCN (Gerakines et al., 2022) and NH_3 (Hudson et al., 2022a) in both amorphous and crystalline forms. We have also studied the vapor pressures of various compounds related to interstellar and solar-system ices, namely propanal by Yarnall et al. (2020), benzene, H_2O, and cyclohexane by Hudson et al. (2022b), and HCN and C_2N_2 by Hudson and Gerakines (2023). We have now used the techniques employed in these recent experiments to measure the vapor pressures of ammonia ice and have adapted them for a study of ammonium cyanide salt at low temperatures.

Here we report the results from measurements of NH_4CN, where we have determined its refractive index, density, IR absorption band strengths, and optical constants at 125 K, and have measured its vapor pressure and enthalpy of sublimation between about 125 and 156 K. We compare our results to vapor pressure measurements dating back to Isambert (1882). We also present measurements of the sublimation enthalpy and vapor pressures of NH_3 near 100 K. The work presented here could aid in identifying and quantifying the amount of NH_4^+ in cometary and interstellar environments, possibly shedding light on other associated species such as cyanide or cyanate anions.

2. LABORATORY METHODS

Samples in this work were created using techniques described in detail in our recent publications. See, e.g., Hudson et al. (2022a) or Hudson et al. (2014). In summary, gases were released into a vacuum chamber and allowed to condense onto a cold substrate (lowest $T \sim 10$ K). For IR transmission measurements, the substrate was made of KBr or CsI. In all cases, samples were grown to thicknesses of up to a few micrometers, measured during film growth by monitoring the intensity of a visible-light laser (λ = 670 nm) passing through the film and substrate at normal incidence (θ = 0°). All IR spectra were collected as 100-scan averages from 5000 to 500 cm^{-1} with a spectrometer resolution of 1 cm^{-1}. For determinations of IR band strengths and optical constants, transmission spectra were measured for 5 samples at different thicknesses, as we have done in similar previous studies (e.g., Hudson et al., 2022a).

To synthesize ammonium cyanide, we followed the methods of Clutter and Thompson (1969). NH_3 and HCN gases were released simultaneously into our vacuum chamber through separate inlet lines while the substrate was held at 125 K. At this temperature, no unreacted molecules remained on the substrate and only their less-volatile reaction product NH_4CN was retained. Each gas was held in a separate glass bulb on a manifold where each was connected to the main vacuum chamber through its own valve. The valves were calibrated and set to deposit each compound at

approximately the same rate. Although the reaction has been shown to occur even at temperatures as low as ~20 K (Gerakines et al., 2004), holding the substrate at 125 K prevented the retention of unreacted NH_3 or HCN. Moreover, the deposition rates chosen (each gas ~1.7 × 10^{15} molecules cm^{-2} s^{-1}) were sufficiently slow to prevent any trapping of unreacted NH_3 or HCN. The resulting NH_4CN sample was seen to grow at a rate of ~3.5 μm hr^{-1} (~1.5 × 10^{15} molecules cm^{-2} s^{-1}), and no evidence of other compounds was noted in the sample.

For refractive index, density, and sublimation rate measurements, we used the same experimental setup described in our previous studies (e.g., Hudson et al. 2017; Hudson et al. 2022b). In summary, the substrate was the gold-coated surface of a quartz-crystal microbalance (QCM) from Inficom attached to the end of the cold finger of a cryostat (ARS Displex) inside an ultra-high vacuum (UHV) chamber (P ~ 10^{-10} Torr). The QCM can be cooled to about 15 K and heated to room temperature with a resistive heater. Our system also included a thermal shroud/radiation shield at ~35 K surrounding the cold finger and most of the microbalance holder, and the sublimating gases condensed upon it, preventing pressure from building up in the system and any gas recondensation. Measured QCM frequencies have a manufacturer's specified uncertainty of 0.1 Hz. Two visible-light (670 nm) lasers were pointed at the substrate with incidence angles of 7° and 55°. Refractive index n was determined by combining information from the interference fringes of the two lasers reflected from the sample during film growth. Briefly, for a sample whose thickness is increasing at a constant rate, the refractive index n_{670} can be determined from the oscillation periods in each laser's interference fringes

$$n_{670} = \sqrt{\frac{\sin^2\theta_2 - (t_1/t_2)^2 \sin^2\theta_1}{1-(t_1/t_2)^2}} \quad (1)$$

where θ_1 and θ_2 are the laser incidence angles and t_1 and t_2 are the measured periods. At the same time, we also monitored the change in frequency of the QCM to determine the sample's density ρ using

$$\rho = \frac{\kappa}{h}\left(\frac{1}{f} - \frac{1}{f_0}\right) \quad (2)$$

where f and f_0 are the frequencies with and without a sample present at the same temperature, h is the sample thickness, and κ is a constant equal to 4.417×10^5 g cm^{-2} Hz that is related to the crystal properties (Lu and Lewis, 1972).

Vapor pressures were determined as described in our recent studies of propanal (Yarnall et al. 2020) and benzene (Hudson et al., 2022b). In summary, we created NH_4CN samples on the QCM substrate at 125 K as already described, and each sample was heated at 1 K min^{-1} while recording the temperature and frequency of the QCM every 2 s until the sample was completely sublimed. Combining the temperature and frequency data with the frequencies of the bare QCM (with no sample) at the same temperatures, the mass per unit area on the substrate at each time step was determined. Subsequently, the sublimation rate (in molecules cm^{-2} s^{-1}) at each temperature was determined from the time derivative of the mass data. Vapor pressures at each temperature were found from the sublimation rates. More details are provided in the next section since the treatment for NH_4CN is not the same as that for NH_3, and the difference requires special discussion and attention.

Ammonia (research grade; MilliporeSigma) was used as obtained by the manufacturer. HCN was prepared from the reaction of potassium cyanide (KCN) and stearic acid (octadecanoic acid) as described in our previous studies of HCN (Gerakines et al., 2004, 2022).

3. RESULTS

3.1 Infrared transmission spectra

The mid-infrared spectrum of an NH_4CN sample with a thickness of 0.43 μm is shown in Fig. 1, created as described in the previous section. Fig. 1 also contains

reference spectra for NH_3 and HCN, whose absorption features are absent from the sample's spectrum. Fig. 2 shows the spectrum of a thicker sample in the region of the short-wavelength feature near 4200 cm^{-1} (2.381 μm), which is too small to appear on the vertical scale for the sample in Fig. 1.

Positions of the three strongest IR absorption features are listed in Table 1, along with their assignments. The NH_4CN transmission spectra we obtained are in good qualitative agreement with the reflection spectra published by Clutter and Thompson (1969), by us in a study of the radiation chemistry of HCN-containing ices (Gerakines et al., 2004), and by Noble et al. (2013). Raman spectra showing similar features were also reported by Kanesaka et al. (1984).

3.2 Refractive index and density

We also measured the refractive index at 670 nm (n_{670}) and density (ρ) of NH_4CN at 125 K, since these properties are needed for the determination of IR band strengths and optical constants. We have recently published similar measurements for a variety of ices, for example as reported by Hudson et al. (2022a) for NH_3, and we refer the reader to these works for a more detailed discussion of the methods and analyses. Three independent measurements were made as described in the previous section, yielding averages of n_{670} = 1.55 ± 0.02 and ρ = 1.10 ± 0.01 g cm^{-3} for NH_4CN at 125 K. The result for ρ agrees with the density of 1.11 g cm^{-3} reported by Lely and Bijvoet (1944) for NH_4CN at 193 K, but our result for its refractive index seems to be the first to be reported.

3.3 IR band strengths and optical constants

We measured the band strengths of NH_4CN features following the procedures described in previous publications (e.g., Gerakines et al., 2022), so only a summary appears here. Having determined the refractive index of NH_4CN, n_{670}, we created several samples over a range of thickness h. From their IR absorbance spectra (shown

in Fig. 3), the peak heights and areas were recorded for the selected features. Beer's Law plots of peak absorbance and integrated absorbance as a function of *h* for each sample (Fig. 4) gave apparent absorption coefficients (α') and apparent band strengths (A') according to the equations

$$Absorbance = \left(\frac{\alpha'}{\ln 10}\right) h \quad (3)$$

$$\int_{band}(Absorbance)\, d\tilde{\nu} = \left(\frac{\rho_N A'}{ln10}\right) h \quad (4)$$

where $\tilde{\nu}$ is the wavenumber (in cm^{-1}), ρ_N is the measured number density (in molecules cm^{-3}), and the factor of ln10 converts absorbance to optical depth. Slopes of the linear fits in Fig. 4 for each IR band were used to find the values of α' and A' listed in Table 1. Uncertainties in the measured values of α' and A' were determined from the uncertainties in the fitted slopes (e.g., Hudson et al., 2017).

Optical constants of NH_4CN (*n* and *k*, the magnitudes of the real and imaginary parts of its complex refractive index) were calculated from the measured IR spectra using the algorithm and software published by Gerakines and Hudson (2020). The values of *n* and *k* were found for five separate NH_4CN samples with different thicknesses and then averaged to produce the final results, which are plotted in Fig. 5. Standard errors in *n* and *k* due to the averaging process were < 0.07 at all wavenumbers, with the highest value located at the 1436 cm^{-1} spectral peak, 0.02 at the 2093 cm^{-1} peak, and 0.01 at the peaks in the 3400-2410 cm^{-1} region. Baseline uncertainties were ~200 times smaller.

3.4 Vapor pressures and enthalpy changes

It is important to appreciate that the result of heating NH_4CN, a salt, in our vacuum systems was different from the result of heating a covalent compound such as NH_3, ammonia. The two changes are shown in the reactions below.

$$NH_3(s) \rightarrow NH_3(g) \quad (5)$$

$$NH_4CN(s) \rightarrow NH_3(g) + HCN(g) \quad (6)$$

The first reaction (Eq. 5) is a conventional sublimation, the conversion of a solid into a gas. As solid NH_3 is warmed, the pressure from the NH_3 product at each temperature is solid NH_3's vapor pressure, with $\Delta_{subl}H$ as the corresponding enthalpy change for the sublimation.

The second reaction above (Eq. 6), although sometimes called a sublimation, is a dissociation. As an ammonium salt, such as the NH_4CN, is heated, a pressure rise results, but from a chemical reaction as opposed to simply a phase change of the initial material. Nevertheless, some authors consider this a sublimation, with the resulting pressure change to be the original salt's vapor pressure, and the corresponding enthalpy change is taken as the sublimation enthalpy. See Luft (1955) for an example of this practice, which we follow. However, we recognize that others have used "dissociation pressure" for the pressure change on heating an ammonium salt (e.g., Ramsay and Young, 1886).

As our previous work on vapor pressures involved covalent compounds, as opposed to ionic ones, here we first present new results on NH_3 followed by our vapor pressure measurements for NH_4CN.

3.4.1 Ammonia

Solid NH_3 was prepared and its vapor pressure and enthalpy change on warming were measured with the procedure described in Yarnall et al. (2020), Hudson et al. (2022b), and Hudson and Gerakines (2023), a procedure resembling that of earlier studies using a QCM by Bryson et al. (1974) and Luna et al. (2012). In summary, solid NH_3 was condensed onto our QCM substrate by conventional vapor-phase deposition and warmed at ~1 K min^{-1} while the QCM frequency and temperature were recorded

every 2 seconds. We used the frequency at each time/temperature to calculate the mass per unit area (μ) of the sample from Eq. (7)

$$\mu = \kappa \left(\frac{1}{f} - \frac{1}{f_0} \right) \tag{7}$$

where f, f_0, and κ have the same definitions as in Eq. (2). The flux of sublimating NH_3 molecules F at time t was found by calculating the rate of change in μ from

$$F = -\frac{1}{m} \frac{d\mu}{dt} \tag{8}$$

where m is the mass of one NH_3 molecule. The corresponding vapor pressure (P) of NH_3 was calculated using the kinetic-theory relation

$$P = F\sqrt{2\pi m k T} \tag{9}$$

where k is the Boltzmann constant. A Clausius-Clapeyron graph of ln(P) vs. 1 / T, according to

$$\ln(P) = (-\Delta_{subl}H^{\theta} / R)(1 / T) + (\text{constant}) \tag{10}$$

resulted in Eq. (11) below, the constants being averages from fitting the data from four separate samples

$$\ln(P / \text{Torr}) = (-3719\ \text{K}) \left(\frac{1}{T} \right) + 22.07 \tag{11}$$

The slope ($-\Delta_{subl}H^{\theta} / R$) of this equation yields the enthalpy of sublimation of solid NH_3, $\Delta_{subl}H^{\theta}$ = 30.92 kJ mol^{-1}. Correlation coefficients were > 0.99 for each ice examined. Propagating the uncertainties of 0.1 Hz in the QCM frequency measurements and 0.1 K

in the temperature measurements leads to an uncertainty < 0.5% for the fit parameters and for $\Delta_{subl}H^{\theta}(NH_3)$.

3.4.2 Ammonium cyanide

Turning to NH_4CN, each mole of NH_4CN decomposing will form two moles of gas-phase product (i.e., NH_3 and HCN), and each product will have a molecular flux equal to that of the NH_4CN decomposed. Luft (1955) correctly described the changes in such ammonium salts by combining and rearranging the standard relations $\Delta_{subl}G^{\theta} = -R\,T \ln K_{eq}$ and $\Delta_{rxn}G^{\theta} = \Delta_{subl}H^{\theta} - T\,\Delta_{rxn}S^{\theta}$ to give

$$\ln(K_{eq}) = (-\Delta_{subl}H^{\theta} / R)(1 / T) + (\Delta_{subl}S^{\theta} / R) \quad (12)$$

where K_{eq} is the equilibrium constant, $\Delta_{rxn}G^{\theta}$ is the change in the Gibbs free energy of the reaction, and $\Delta_{rxn}S^{\theta}$ is the change in the entropy. In the case of NH_4CN decomposition, $K_{eq} = P_{NH3}P_{HCN}$ or just

$$K_{eq} = P^2 \quad (13)$$

since $P_{NH3} = P_{HCN}$. Substituting this K_{eq} into Eq. (12) for $\ln(K_{eq})$ and rearranging gives

$$\ln(P) = (-\Delta_{subl}H^{\theta} / 2R)(1/ T) + (\Delta_{subl}S^{\theta} / 2R) \quad (14)$$

Note particularly the factor of 2 in the coefficient of (1 / *T*). A graph of ln(*P*) as a function of 1 / *T* will give a reaction energy only if that same factor of 2 is used with the graph's slope. The pressure *P* is the value that NH_4CN would produce were it to undergo sublimation without decomposing.

Returning again to our own work, samples of NH_4CN were synthesized on our QCM's surface, as already described, and then warmed while recording temperature and QCM frequency. Conversions of the data to pressures were made as with our NH_3

measurements. A plot of ln(P) vs. 1/T was prepared for each NH_4CN sample, and data points in the range of 135-156 K (the linear part of the trend, with correlation coefficients > 0.99) were fit using a linear least-squares analysis. Averaging results from four samples gave

$$\ln(P/Torr) = (-5104\ \mathrm{K})\left(\frac{1}{T}\right) + 21.65 \quad (15)$$

The slope of –5104 K = $-\Delta_{rxn}H^{\theta}$ / (2R) gave $\Delta_{rxn}H^{\theta}$ = 84.87 kJ mol^{-1} for NH_4CN decomposition into NH_3 and HCN. Data for one of our NH_4CN samples are shown in Fig. 6. As described above for ammonia, propagating the uncertainties of 0.1 Hz in the QCM frequency measurements and 0.1 K in the temperature measurements leads to an uncertainty < 0.5% for the fit parameters and for $\Delta_{rxn}H^{\theta}(NH_4CN)$.

Our new results for NH_3 and NH_4CN are listed in Table 2, along with results for HCN as reported recently by Hudson and Gerakines (2023) and H_2O from Hudson et al. (2022b) for comparison. Table 3 lists the vapor pressures for NH_3 and NH_4CN over the temperature ranges where the sublimation rates were measured in this work. The sublimation rate vs. temperature curves from the fits to the data for all four compounds from Table 2 are plotted in Fig. 7. It can be seen that the sublimation rate of NH_4CN is lower than that of both NH_3 and HCN and higher than that of H_2O at every temperature.

Before discussing our results, a few additional points should be mentioned. The first concerns our assumption that the warming of NH_4CN under vacuum gives complete dissociation of the compound into NH_3 and HCN. The mechanism for such changes in ammonium salts has been explored by Zhu et al. (2007) and can be applied to NH_4CN. Those authors quantum mechanically modeled sublimation in crystalline NH_4Cl as following a sequence in which NH_4^+ / Cl^- ion pairs begin to break away from the solid to a so-called relaxed state, followed by co-sublimation of the ion pair and then rapid gas-phase H^+ transfer to give NH_3 and HCl, the process leading to complete dissociation. The same authors calculated the overall energy change for the process and found it to agree with the measured value. We envision a similar set of steps for NH_4CN

sublimation. As support, we note the non-detection of NH_4CN^+ by mass spectrometry both in our work and that of Noble et al. (2013). See also the non-detection of the parent cation in the ammonium chloride experiments of Goldfinger and Verhaegan (1969) and of Hänni et al. (2019).

A different argument for complete dissociation of NH_4CN comes from the relative proton affinity of the anions in NH_4Cl and NH_4CN. Since HCN is a weaker acid than HCl, one expects that the conjugate base CN^- is stronger than Cl^-, which implies an even greater extent of H^+ transfer from the NH_4^+ cation on subliming NH_4CN, to give NH_3 and HCN, compared to NH_4Cl, to give NH_3 and HCl. The conclusion is that if NH_4Cl undergoes complete dissociation on warming, then NH_4CN certainly will.

Another concern relating to our measurements is the possibility that some of the gas-phase NH_3 and HCN molecules produced on warming NH_4CN might redeposit onto our QCM's surface, changing our measured QCM frequencies and, in turn, our sublimation fluxes and vapor pressures. This complication seems unlikely due to the low gas-phase pressures in our vacuum system before and after warming the substrate (i.e., QCM surface). We also note that our QCM is surrounded by a stainless-steel radiation shroud at ~35 K, which effectively traps NH_3 and HCN, reducing their gas-phase abundance even more.

A final point involves the differences in vapor pressures and sublimation energies that might accompany different measurements methods, specifically a sample chamber that is closed compared to one that is under ultra-high vacuum. No such difference should be seen in vapor pressures arising from the sublimation from our QCM surface, resulting in a somewhat less complex measurement than that in conventional studies of properties in closed containers (e.g., bomb calorimeters). This has been pointed out in the classic sublimation study of Langmuir (1913) and in more recent work, such as that of Bryson et al. (1974). As additional support, see also our measurements of the vapor pressures of crystalline H_2O-ice, which are in excellent agreement with the best results from a variety of techniques (Bryson et al., 1974; Wagner et al., 2011). Finally,

measurements by multiple methods, including the QCM method used here, have been shown to give similar sublimation energies (Luna et al., 2014).

4. DISCUSSION

4.1 IR band strengths of ammonium cyanide

The band strengths for the IR features of NH_4^+ and CN^- at 125 K resulting from our work are listed in Table 1. Few measurements exist in the literature for direct comparison, and the literature that does exist on the IR band strengths of NH_4^+ suffers from a myriad of issues. Schutte and Khanna (2003) reported a band strength for the IR absorption of NH_4^+ at 1436 cm^{-1} of $A' = 4.4 \times 10^{-17}$ cm molecule^{-1} with a "factor of two" (100%) uncertainty. Their method was to monitor the growth of the NH_4^+ feature that resulted when ammonium formate (NH_4COOH) was produced in ice mixtures of NH_3 + formic acid (HCOOH) held at 80 and 120 K. The corresponding column densities of NH_4^+ (needed for finding its band strength) were assumed to be the same as that of the NH_3 consumed in the acid-base reaction, determined from the loss of the NH_3 band area together with a band strength from d'Hendecourt and Allamandola (1986). This result contains assumptions and unknowns, making a direct comparison difficult, if not impossible. The method chosen assumed that the band strength for NH_3 mixed with formic acid and H_2O at 120 K was the same as that of amorphous NH_3 at 10 K, which also was assumed to have a density of 1 g cm^{-3}. Moreover, no IR spectra of the samples in the acid-base reaction experiments were shown. Their experiments at 80 and 120 K resulted in different values for A', but the 120-K value was adopted without justification, and it is not clear if more than two experiments were conducted to test the reproducibility of their results. The uncertainty of 100% was described as "standard", without statistical justification or evidence. Despite the problems outlined above, recent results from the James Webb Space Telescope (McClure et al., 2023) cite these band strengths for calculating column densities of NH_4^+ in the ISM. Our measurements of A' contain no assumptions, and all required information about the samples (refractive

index, mass density, and IR spectra) are presented in this report and were measured in our laboratory for samples under appropriate conditions.

Noble et al. (2013) reported a band strength for the 2093 cm^{-1} feature of CN^- of $A' = (1.8 \pm 1.5) \times 10^{-17}$ cm molecule^{-1}, ~200% larger than our result listed in Table 1. Their value was based on IR spectra measured in reflectance, where the use of band strengths is not necessarily correct because of the non-linearity of band areas with sample thickness. Moreover, their method of determining A' also relied on scaling with large uncertainties, leading to the high relative uncertainty that they report (see the explanation in their text for details).

4.2 Enthalpy of sublimation for ammonium cyanide

The two most recent sets of vapor pressure results for NH_4CN in the literature are those of Stull (1947) and Luft (1955), and each set rests on measurements from the 19th century. Stull used the vapor-pressure data of Isambert (1882), which was limited to about 7 - 17 °C, and extrapolated it over two additional orders of magnitude of pressure. His analysis was used later to derive an enthalpy of vaporization for NIST's Chemistry WebBook (Acree and Chickos, 2023; https://webbook.nist.gov/). The noun vaporization is somewhat misleading as no liquid is formed on warming NH_4CN in the temperature range of either Stull or Isambert, but the more serious concern is that the listed value of $\Delta_{rxn}H^{\theta}(NH_4CN) = 47.1$ kJ mol^{-1} appears to have been derived without considering the factor of 2 already mentioned (see Eq. 14).

Luft (1955) determined $\Delta_{rxn}H^{\theta}(NH_4CN)$ through a different approach. Literature values of ΔH^{θ} and ΔS^{θ} for the formation of NH_4CN, NH_3, and HCN were combined according to

$$\Delta_{rxn}H^{\theta} = \Delta_f H^{\theta}_{NH3(g)} + \Delta_f H^{\theta}_{HCN(g)} - \Delta_f H^{\theta}_{NH4CN(s)} \quad (16)$$

to give the enthalpy change for NH_4CN decomposition, which Luft called NH_4CN sublimation. A similar equation gave the corresponding entropy change, $\Delta_{rxn}S^{\theta}$. The author then used

$$\ln(P) = (-\Delta_{rxn}H^{\theta} / 2R)(1 / T) + (\Delta_{rxn}S^{\theta} / 2R) \quad (17)$$

to calculate vapor pressures. Unfortunately, neither the value of $\Delta_{rxn}S^{\theta}$ Luft used, nor the details of the method to find it, were supplied. For $\Delta_{rxn}H^{\theta}$, a reference was made to National Bureau of Standards (NBS) tables that, in turn, cited Berthelot (1875), but details again were not given. The formation enthalpy Luft gave for NH_4CN is $\Delta_f H^{\theta}$ = 0.0 kcal mol^{-1} = 0.0 kJ mol^{-1}, which could be correct, but seems suspiciously small compared to that for other ammonium salts, such as -314.55 kJ mol^{-1} for NH_4Cl reported by Chase (1998). Luft's $\Delta_{rxn}H^{\theta}(NH_4CN)$ = 84.5 kJ mol^{-1} is in NIST's Chemistry WebBook, where it is labeled a sublimation enthalpy. Although Luft's value is strikingly close to our own 84.80 kJ mol^{-1}, the unknowns and omissions in his work make it impossible to determine if the agreement is anything but serendipitous. His nomogram for calculating vapor pressures is restricted to about 293 - 333 K (20 - 60 °C), temperatures far above the 135 - 156 K of interest here. Finally, the results he uses from Berthelot (1875) appear to be based on reactions with HCN and NH_3 dissolved in water, not reactions under vacuum conditions.

We conclude from this examination of the literature that our vapor pressures and enthalpy change for NH_4CN are the first of their type in which all steps are described, and anhydrous conditions and vacuum chambers are used, with no reliance on 19th-century results.

The desorption energy of NH_4CN was reported by Noble et al. (2013) to be 38.0 ± 1.4 kJ mol^{-1}, which they determined in a temperature-programmed desorption (TPD) experiment. Since no signals were detected at m/z = 43 or 44 due to NH_4CN, it was assumed that the salt completely dissociated into NH_3 and HCN before sublimation, and

Noble et al. fit the trace of the HCN mass-spectrometric signal at m/z = 27 Da with zeroth-order desorption kinetics. Note that their reported desorption energy value is less than half of the enthalpy change reported by us and by Isambert (1882). NH_4CN was assumed to desorb directly into NH_3 + HCN, and so the abundance of HCN detected in the gas should equal the amount of NH_4CN sublimated. The derived value also depended on an assumed "pre-exponential" factor in the kinetic equation for the desorption rate (see their Eq. 2), and the result was shown to vary (by 6-7%) according to the value chosen for this factor. Our method of using a QCM to directly measure the mass lost during sublimation does not require any such assumptions.

Our QCM experimental technique is similar to that of TPD, in that we monitor the mass per unit area lost as a sample is heated at a constant rate. Therefore, we performed a TPD-style analysis on our data. The flux values (in molecules cm^{-2} s^{-1}) from Fig. 6c were converted to molecules lost per unit area per unit temperature (molecules cm^{-2} K^{-1}) by dividing by our heating rate (1 K min^{-1}). A graph of the resulting data followed a zeroth-order desorption curve given by a simple exponential $A\exp(-E_a/RT)$, where A is a pre-exponential factor, and E_a is the desorption energy. Our values measured between 134 and 155 K were fit with this function, resulting in best-fitting parameters of $A = 3.22\times10^{28}$ molecules cm^{-2} K^{-1} and $E_a = 43.13$ kJ mol^{-1}. Note that this energy is similar to that by Noble et al. (2013) and approximately half of our reported value for $\Delta_{subl}H$.

Our fundamental measurement using the QCM technique is the sublimation flux of NH_4CN at each temperature, which is then converted to a pressure using Eq. (9). While the measurement does not take place in an equilibrium environment, such a flux through an arbitrary surface corresponds to a pressure, which in this case is equivalent to the vapor pressure, as if the ice sample were contained within the volume of a Knudsen effusion cell where the gas is released through a small pinhole at the measured flux (Langmuir 1913). In non-equilibrium environments such as the ISM or for cometary sublimation processes, the sublimation flux may be the most-

relevant parameter along with determinations of desorption order and energy of desorption (as determined from TPD experiments, see e.g. Minissale et al., 2022).

4.3 Fits to pressure vs. temperature data

Pressure vs. temperature data for NH_3 at ~175-200 K were reported by Overstreet and Giauque (1937), who also reported a Clausius-Clapeyron fit yielding $\Delta_{subl}H_.$ = 31.22 kJ mol^{-1}, a ~1% difference from our value of 30.92 kJ mol^{-1} (Table 3). The solid NH_3 data from Overstreet and Giauque (1937) are plotted in Fig. 8 along with our measurements at 95-115 K. To link the two data sets, we used the Cox equation (Cox 1936) as we have done in previous studies for other compounds (Hudson et al., 2022b, Hudson and Gerakines, 2023). A least-squares fit gave

$$\ln\left(\frac{P}{P_0}\right) = \left(1 - \frac{T_0}{T}\right)\exp(A_0 + A_1 T + A_2 T^2) \quad (18)$$

with A_0 = 2.6965, A_1 = 4.7754×10^{-3} K^{-1}, and A_2 = -1.8442×10^{-5} K^{-2}, and where the triple point temperature and pressure (T_0 = 195.36 K, P_0 = 45.58 Torr) were taken from Overstreet and Giauque (1937). Also plotted in Fig. 8 is the low-temperature extrapolation suggested by Fray and Schmitt (2009), which overestimates the pressures by ~50-75% as compared to the laboratory measurements.

For NH_4CN, the pressures measured by Isambert (1882) for temperatures in the range of 280-290 K are plotted in Fig. 9 along with our data for 135-155 K listed in Table 3. The extrapolated values reported by Stull (1947) are also shown. As described for NH_3, these two data sets were linked using a fit to the Cox equation (Eq. 10), where the temperature and pressure of T_0 = 290.4 K and P_0 = 326.2 Torr as measured by Isambert were used as the anchor points in lieu of the triple-point values. The best-fitting curve is shown in Fig. 9 and has the coefficients A_0 = 2.4722, A_1 = 5.5227×10^{-3} K^{-1}, and A_2 = -1.4868×10^{-5} K^{-2}.

5. SUMMARY AND APPLICATIONS

The refractive index, density, infrared band strengths, and infrared optical constants of ammonium cyanide at 125 K have been measured. Sublimation fluxes, vapor pressures, and enthalpy of sublimation of NH_4CN from 135 to 155 K also have been reported, representing some of the first such measurements for this compound in over 140 years. The vapor pressures and enthalpy of sublimation for NH_3 from 95 to 115 K have also been measured. It was noted that the dissociation of the subliming salt requires a different treatment than for a non-dissociating compound such as ammonia, and it was found that there are inconsistencies in the way that the sublimation enthalpy for NH_4CN has been reported in the literature.

The physical and spectroscopic properties of NH_4CN reported here can be used to understand observations of Solar-System bodies such as comet 67P/Churyumov-Gerasimenko or other icy objects that contain NH_4^+ salts. IR spectral data and IR band strengths have also been provided to better understand the interstellar absorption features near 7 μm suspected to be due in part to NH_4^+.

Another possible application of this work has to do with the outgassing of cometary NH_3. As a comet approaches the Sun in its orbit, different gases are expected in its coma as a result of ice sublimation. The comparison in Fig. 7, which includes new data for both ammonia and NH_4CN, may represent the order, from low temperature to high, in which NH_3, HCN, NH_4CN, and H_2O would sublime directly from the surface of a comet nucleus. The contribution of ammonium cyanide to the HCN or NH_3 observed around comets would become apparent only at smaller heliocentric distances than expected for single-component ices. NH_4CN sublimating from dust particles may also provide a source of the NH_3, whose emission is observed for many comets and has been correlated with HCN in some cases (e.g., by Dello Russo et al., 2016).

The authors wish to thank Michael J. Mumma for fruitful discussions that motivated this study. Gregory Girolami and Vera Mainz of the University of Illinois are thanked for the information they found and provided about F. Isambert, his publications, and his experiments. We also thank the Donald F. & Mildred Topp Othmer Library of Chemical History at the Science History Institute for assistance in obtaining some of the reference materials. We acknowledge support from the NASA Astrophysics Research and Analysis (APRA) and Planetary Data Archiving, Restoration, and Tools (PDART) Programs, as well as NASA's Planetary Science Division Internal Scientist Funding Program through the Fundamental Laboratory Research (FLaRe) work package at the NASA Goddard Space Flight Center.

ORCID iDs
Perry A. Gerakines https://orcid.org/0000-0002-9667-5904
Yukiko Y. Yarnall https://orcid.org/0000-0003-0277-9137
Reggie L. Hudson https://orcid.org/0000-0003-0519-9429

DATA AVAILABILITY

All data, including IR spectra and optical constants are available on our website (http://science.gsfc.nasa.gov/691/cosmicice).

REFERENCES

Acree, W. E., Chickos, J. S., 2023, "Phase Transition Enthalpy Measurements of Organic and Organometallic Compounds" in: *NIST Chemistry WebBook, NIST Standard Reference Database Number 69*, Eds. P.J. Linstrom and W.G. Mallard, National Institute of Standards and Technology, Gaithersburg MD, 20899, https://doi.org/10.18434/T4D303, (retrieved February 9, 2024).

Altwegg, K., Balsiger, H., Hanni, N., Rubin, M., Schuhmann, M., Schroeder, I., Semon, T., Wampfler, S., Berthelier, J. J., Briois, C., Combi, M., Gombosi, T. I., Cottin, H., De Keyser, J., Dhooghe, F., Fiethe, B., Fuselier, S. A., 2020. Evidence of ammonium salts in comet 67P as explanation for the nitrogen depletion in cometary comae. Nat Astron 4, 533-540. doi: 10.1038/s41550-019-0991-9

Altwegg, K., Combi, M., Fuselier, S. A., Hänni, N., De Keyser, J., Mahjoub, A., Müller, D. R., Pestoni, B., Rubin, M., Wampfler, S. F., 2022. Abundant ammonium hydrosulphide embedded in cometary dust grains. Mon. Not. R. Astron. Soc. 516, 3900-3910. doi: 10.1093/mnras/stac2440

Berthelot, M., 1875. Recherches thermochimiques sur la série du cyanogène. Annales de Chimie et de Physique, 5^{e} série, 433-492.

Boogert, A. C. A., Gerakines, P. A., Whittet, D. C. B., 2015. Observations of the icy universe. Annual Review of Astronomy and Astrophysics 53, 541-581. doi: 10.1146/annurev-astro-082214-122348

Bryson III, C. E., Cazcarra, V., Levenson, L. L., 1974. Sublimation rates and vapor pressures of H_2O, CO_2, N_2O, and Xe. J. Chem. Eng. Data 19, 107-110. doi: 10.1021/je60061a021

Chase, M.W., Jr., *NIST-JANAF Themochemical Tables, Fourth Edition*, J. Phys. Chem. Ref. Data, Monograph 9, 1998, p. 765.

Clutter, D. R., Thompson, W. E., 1969. Infrared spectroscopic study of polycrystalline NH_4CN. J. Chem. Phys. 51, 153-159. doi: 10.1063/1.1671702

Cook, J. C., Ore, C. M. D., Protopapa, S., Binzel, R. P., Cartwright, R., Cruikshank, D. P., Earle, A., Grundy, W. M., Ennico, K., Howett, C., Jennings, D. E., Lunsford, A. W., Olkin, C. B., Parker, A. H., Philippe, S., Reuter, D., Schmitt, B., Stansberry, J. A., Alan Stern, S., Verbiscer, A., Weaver, H. A., Young, L. A., 2018. Composition of Pluto's small satellites: Analysis of New Horizons spectral images. Icarus 315, 30-45. doi: 10.1016/j.icarus.2018.05.024

Cox, E. R., 1936. Hydrocarbon vapor pressures. Industrial & Engineering Chemistry 28, 613-616. doi: 10.1021/ie50317a029

Dello Russo, N., Kawakita, H., Vervack, R. J., Weaver, H. A., 2016. Emerging trends and a comet taxonomy based on the volatile chemistry measured in thirty comets with high-resolution infrared spectroscopy between 1997 and 2013. Icarus 278, 301-332. doi: 10.1016/j.icarus.2016.05.039

De Sanctis, M. C., Ammannito, E., Raponi, A., Frigeri, A., Ferrari, M., Carrozzo, F. G., Ciarniello, M., Formisano, M., Rousseau, B., Tosi, F., Zambon, F., Raymond, C. A., Russell, C. T., 2020. Fresh emplacement of hydrated sodium chloride on Ceres from ascending salty fluids. Nat Astron 4, 786-793. doi: 10.1038/s41550-020-1138-8

Fastelli, M., Comodi, P., Maturilli, A., Zucchini, A., 2020. Reflectance spectroscopy of ammonium salts: Implications for planetary surface composition. Minerals 10, 902. doi: 10.3390/min10100902

Fray, N., Schmitt, B., 2009. Sublimation of ices of astrophysical interest: A bibliographic review. Planet. Space Sci. 57, 2053-2080. doi: 10.1016/j.pss.2009.09.011

Gerakines, P. A., Moore, M. H., Hudson, R. L., 2004. Ultraviolet photolysis and proton irradiation of astrophysical ice analogs containing hydrogen cyanide. Icarus 170, 202-213. doi: 10.1016/j.icarus.2004.02.005

Gerakines, P. A., Hudson, R. L., 2015. First infrared band strengths for amorphous CO_2, an overlooked component of interstellar ices. Astrophys. J. Letters 808, L40. doi: 10.1088/2041-8205/808/2/L40

Gerakines, P. A., Yarnall, Y. Y., Hudson, R. L., 2022. Direct measurements of infrared intensities of HCN and H_2O + HCN ices for laboratory and observational astrochemistry. Mon. Not. R. Astron. Soc. 509, 3515-3522. doi: 10.1093/mnras/stab2992

Goldfinger, P., Verhaegen, G., 1969. Stability of gaseous ammonium chloride molecule. J. Chem. Phys. 50, 1467-1471. doi: 10.1063/1.1671212

Grim, R., Greenberg, J. M., Schutte, W., Schmitt, B., 1989. Ions in grain mantles - A new explanation for the 6.86-micron absorption in W33A. Astrophys. J. 341, L87-L90. doi: 10.1086/185464

Hänni, N., Gasc, S., Etter, A., Schuhmann, M., Schroeder, I., Wampfler, S. F., Schurch, S., Rubin, M., Altwegg, K., 2019. Ammonium salts as a source of small molecules observed with high-resolution electron-impact ionization mass spectrometry. J. Phys. Chem. A 123, 5805-5814. doi: 10.1021/acs.jpca.9b03534

Hudson, R. L., Loeffler, M. J., Gerakines, P. A., 2017. Infrared spectra and band strengths of amorphous and crystalline N_2O. J. Chem. Phys. 146, 024304. doi: 10.1063/1.4973548

Hudson, R. L., Gerakines, P. A., Moore, M. H., 2014. Infrared spectra and optical constants of astronomical ices: II. Ethane and ethylene. Icarus 243, 148-157. doi: 10.1016/j.icarus.2014.09.001

Hudson, R. L., Gerakines, P. A., Yarnall, Y. Y., 2022a. Ammonia ices revisited: new IR intensities and optical constants for solid NH_3. Astrophys. J. 925, 156. doi: 10.3847/1538-4357/ac3e74

Hudson, R. L., Yarnall, Y. Y., Gerakines, P. A., 2022b. Benzene vapor pressures at Titan temperatures: First microbalance results. Planetary Science Journal, 3, 120. doi: 10.3847/PSJ/ac67a5

Hudson, R. L., Gerakines, P. A., 2023. Infrared spectra and vapor pressures of crystalline C_2N_2, with comparisons to crystalline HCN. The Planetary Science Journal 4, 205. doi: 10.3847/PSJ/ad0040

Isambert, M., 1882. Sur le bisulfhydrate et le cyanhydrate d'ammoniaque. Comptes Rendus 94, 958-960.

Kanesaka, I., Kawahara, H., Kiyokawa, Y., Tsukamoto, M., Kawai, K., 1984. The vibrational spectrum of the ammonia-hydrogen cyanide system and the normal coordinate analysis of NX_4CN (x=h or d). J Raman Spectrosc 15, 327-330. doi: https://doi.org/10.1002/jrs.1250150507

King, T. V. V., Clark, R. N., Calvin, W. M., Sherman, D. M., Brown, R. H., 1992. Evidence for ammonium-bearing minerals on Ceres. Science 255, 1551-1553. doi: 10.1126/science.255.5051.1551

Lacy, J. H., Baas, F., Allamandola, L. J., Persson, S. E., McGregor, P. J., Lonsdale, C. J., Geballe, T. R., Vandebult, C. E. P., 1984. 4.6-micron absorption feature due to solid-phase CO and cyano-group molecules toward compact infrared sources. Astrophys. J. 276, 533-543. doi: 10.1086/161642

Langmuir, I., 1913. The vapor pressure of metallic tungsten. Phys. Rev. 2, 329-342. doi: 10.1103/PhysRev.2.329

Lely, J. A., Bijvoet, J. M., 1944. The crystal structure and anisotropic temperature vibration of ammonium cyanide. Recueil Des Travaux Chimiques Des Pays-Bas 63, 39-43. doi: 10.1002/recl.19440630205

Loeffler, M. J., Moore, M. H., Gerakines, P. A., 2016. The effects of experimental conditions on the refractive index and density of low-temperature ices: Solid carbon dioxide. Astrophys. J. 827, 98. doi: 10.3847/0004-637X/827/2/98

Luft, N. W., 1955. Sublimation pressures and latent heats of ammonium salts. Ind. Chem. 31, 502-504.

Luna, R., Millan, C., Domingo, M., Santonja, C., Satorre, M., 2012. Upgraded sublimation energy determination procedure for icy films. Vacuum 86, 1969-1973. doi: 10.1016/j.vacuum.2012.05.010

Luna, R., Satorre, M. A., Santonja, C., Domingo, M., 2014. New experimental sublimation energy measurements for some relevant astrophysical ices. Astron. Astrophys. 566, A27. doi: 10.1051/0004-6361/201323249

McClure, M. K., Rocha, W. R. M., Pontoppidan, K. M., Crouzet, N., Chu, L. E. U., Dartois, E., Lamberts, T., Noble, J. A., Pendleton, Y. J., Perotti, G., Qasim, D., Rachid, M. G., Smith, Z. L., Sun, F., Beck, T. L., Boogert, A. C. A., Brown, W. A.,

Caselli, P., Charnley, S. B., Cuppen, H. M., Dickinson, H., Drozdovskaya, M. N., Egami, E., Erkal, J., Fraser, H., Garrod, R. T., Harsono, D., Ioppolo, S., Jiménez-Serra, I., Jin, M., Jørgensen, J. K., Kristensen, L. E., Lis, D. C., McCoustra, M. R. S., McGuire, B. A., Melnick, G. J., Öberg, K. I., Palumbo, M. E., Shimonishi, T., Sturm, J. A., van Dishoeck, E. F., Linnartz, H., 2023. An Ice Age JWST inventory of dense molecular cloud ices. Nat Astron 7, 431-443. doi: 10.1038/s41550-022-01875-w

Minissale, M., Aikawa, Y., Bergin, E., Bertin, M., Brown, W. A., Cazaux, S., Charnley, S. B., Coutens, A., Cuppen, H. M., Guzman, V., Linnartz, H., McCoustra, M. R. S., Rimola, A., Schrauwen, J. G. M., Toubin, C., Ugliengo, P., Watanabe, N., Wakelam, V., Dulieu, F., 2022. Thermal desorption of interstellar ices: A review on the controlling parameters and their implications from snowlines to chemical complexity. ACS Earth Space Chem. 6, 597-630. doi: 10.1021/acsearthspacechem.1c00357

Noble, J. A., Theule, P., Borget, F., Danger, G., Chomat, M., Duvernay, F., Mispelaer, F., Chiavassa, T., 2013. The thermal reactivity of HCN and NH_3 in interstellar ice analogues. Mon. Not. R. Astron. Soc. 428, 3262-3273. doi: 10.1093/mnras/sts272

Overstreet, R., Giauque, W. F., 1937. Ammonia. The heat capacity and vapor pressure of solid and liquid. Heat of vaporization. The entropy values from thermal and spectroscopic data. J. Am. Chem. Soc. 59, 254-259. doi: 10.1021/ja01281a008

Poch, O., Istiqomah, I., Quirico, E., Beck, P., Schmitt, B., Theulé, P., Faure, A., Hily-Blant, P., Bonal, L., Raponi, A., Ciarniello, M., Rousseau, B., Potin, S., Brissaud, O., Flandinet, L., Filacchione, G., Pommerol, A., Thomas, N., Kappel, D., Mennella, V., Moroz, L., Vinogradoff, V., Arnold, G., Erard, S., Bockelée-Morvan, D., Leyrat, C., Capaccioni, F., De Sanctis, M. C., Longobardo, A., Mancarella, F., Palomba, E., Tosi, F., 2020. Ammonium salts are a reservoir of nitrogen on a

cometary nucleus and possibly on some asteroids. Science 367, eaaw7462. doi:10.1126/science.aaw7462

Poch, O., Istiqomah, I., Quirico, E., Beck, P., Schmitt, B., Theulé, P., Faure, A., Hily-Blant, P., Bonal, L., Raponi, A., Ciarniello, M., Rousseau, B., Potin, S., Brissaud, O., Flandinet, L., Filacchione, G., Pommerol, A., Thomas, N., Kappel, D., Mennella, V., Moroz, L., Vinogradoff, V., Arnold, G., Erard, S., Bockelée-Morvan, D., Leyrat, C., Capaccioni, F., De Sanctis, M. C., Longobardo, A., Mancarella, F., Palomba, E., Tosi, F., 2023. Identification of ammonium salts on comet 67P/C-G surface from infrared VIRTIS/Rosetta data based on laboratory experiments. Implications and perspectives. in: V. Mennella, C. Joblin, (Eds.), European Conference on Laboratory Astrophysics ECLA2020. Springer International Publishing, Cham, pp. 271-279. doi: 10.1007/978-3-031-29003-9_31

Ramsay, W., Young, S., 1886. II. On evaporation and dissociation. - Part I. Phil. Trans. R. Soc. 177, 71-122. doi: 10.1098/rstl.1886.0003

Schutte, W. A., Khanna, R. K., 2003. Origin of the 6.85 μm band near young stellar objects: The ammonium ion (NH_4^+) revisited. Astron. Astrophys. 398, 1049-1062. doi: 10.1051/0004-6361:20021705

Stull, D. R., 1947. Inorganic compounds. Industrial & Engineering Chemistry 39, 540-550. doi: 10.1021/ie50448a023

Wagner, W., Riethmann, T., Feistel, R., Harvey, A. H., 2011. New equations for the sublimation pressure and melting pressure of H_2O ice Ih. J. Phys. Chem. Ref. Data 40, 043103. doi: 10.1063/1.3657937

Yarnall, Y. Y., Gerakines, P. A., Hudson, R. L., 2020. Propanal, an interstellar aldehyde - first infrared band strengths and other properties of the amorphous and

crystalline forms. Mon. Not. R. Astron. Soc. 494, 4606-4615. doi: 10.1093/mnras/staa1028

Zhu, R. S., Wang, J. H., Lin, M. C., 2007. Sublimation of ammonium salts: A mechanism revealed by a first-principles study of the NH_4Cl system. J. Phys. Chem. C 111, 13831-13838. doi: 10.1021/jp073448w

Zimmer, C., Khurana, K. K., Kivelson, M. G., 2000. Subsurface oceans on Europa and Callisto: Constraints from Galileo magnetometer observations. Icarus 147, 329-347. doi: 10.1006/icar.2000.6456

TABLES

Table 1

Absorption coefficients and apparent band strengths of NH_4CN

Peak position / cm^{-1} (μm)	Description	α' / cm^{-1}	Integration limits / cm^{-1}	A' / 10^{-17} cm $molecule^{-1}$
3023 (3.308)	N-H stretching region	20,260 ± 420	3400-2410	41.4 ± 0.1
2093 (4.778)	CN^- stretching mode	14,030 ± 460	2100-2088	0.574 ± 0.015
1436 (6.964)	NH_4^+ bending mode	35,950 ± 1100	1500-1350	3.58 ± 0.07

Table 2

Clausius-Clapeyron fit parameters and sublimation enthalpies [a]

Compound	Intercept	Slope / K	Sublimation enthalpy, $\Delta_{subl}H$ / kJ mol^{-1}	Reference
H_2O	23.3	-6036	50.2	Hudson et al. (2022b)
HCN	21.61	-4568	37.98	Hudson and Gerakines (2023)
NH_3	22.07 ± 0.36	-3719 ± 5	30.92 ± 0.04	This work
NH_4CN	21.65 ± 0.01	-5104 ± 1	84.80 ± 0.02	This work

[a] Results of fitting ln(P) vs. 1/T (see text).

Table 3

Vapor pressures of NH_3 and NH_4CN [a]

T / K	NH_3 Vapor pressure / 10^{-6} Torr	T / K	NH_4CN Vapor pressure / 10^{-6} Torr
95	0.03832	135	0.09708
100	0.2713	140	0.3742
105	1.594	145	1.314
110	7.976	150	4.244
115	34.69	155	12.71

[a] Pressures calculated using the fit parameters listed in **Table 2**.

FIGURES

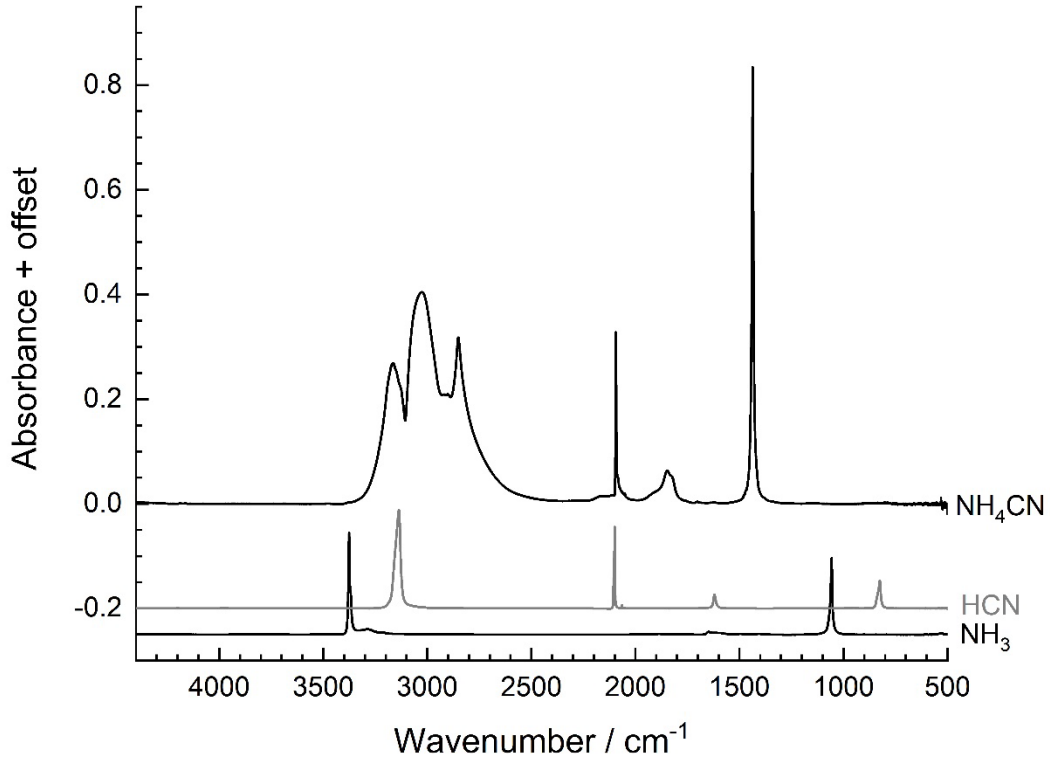

Fig. 1. The IR spectrum of NH_4CN created at 125 K from the co-deposition of NH_3 and HCN to a thickness of 0.432 μm (top). The IR spectra of HCN at 120 K (middle) and NH_3 at 100 K (bottom) are shown for reference. Spectra are offset for clarity.

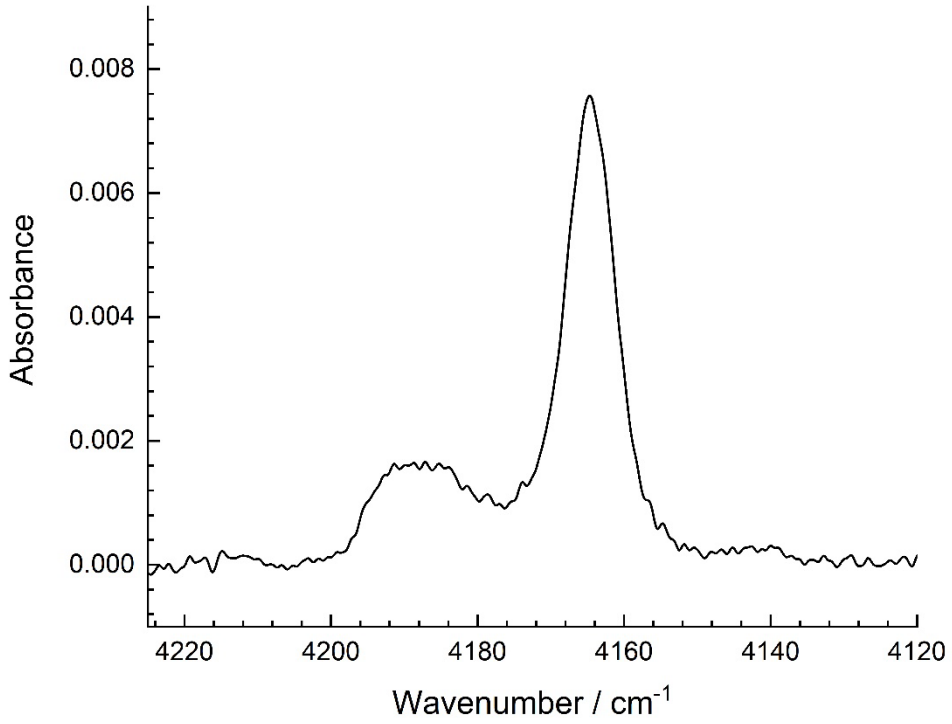

Fig. 2. The IR spectrum of a sample of NH_4CN created at 125 K and grown to a thickness of 3.46 μm.

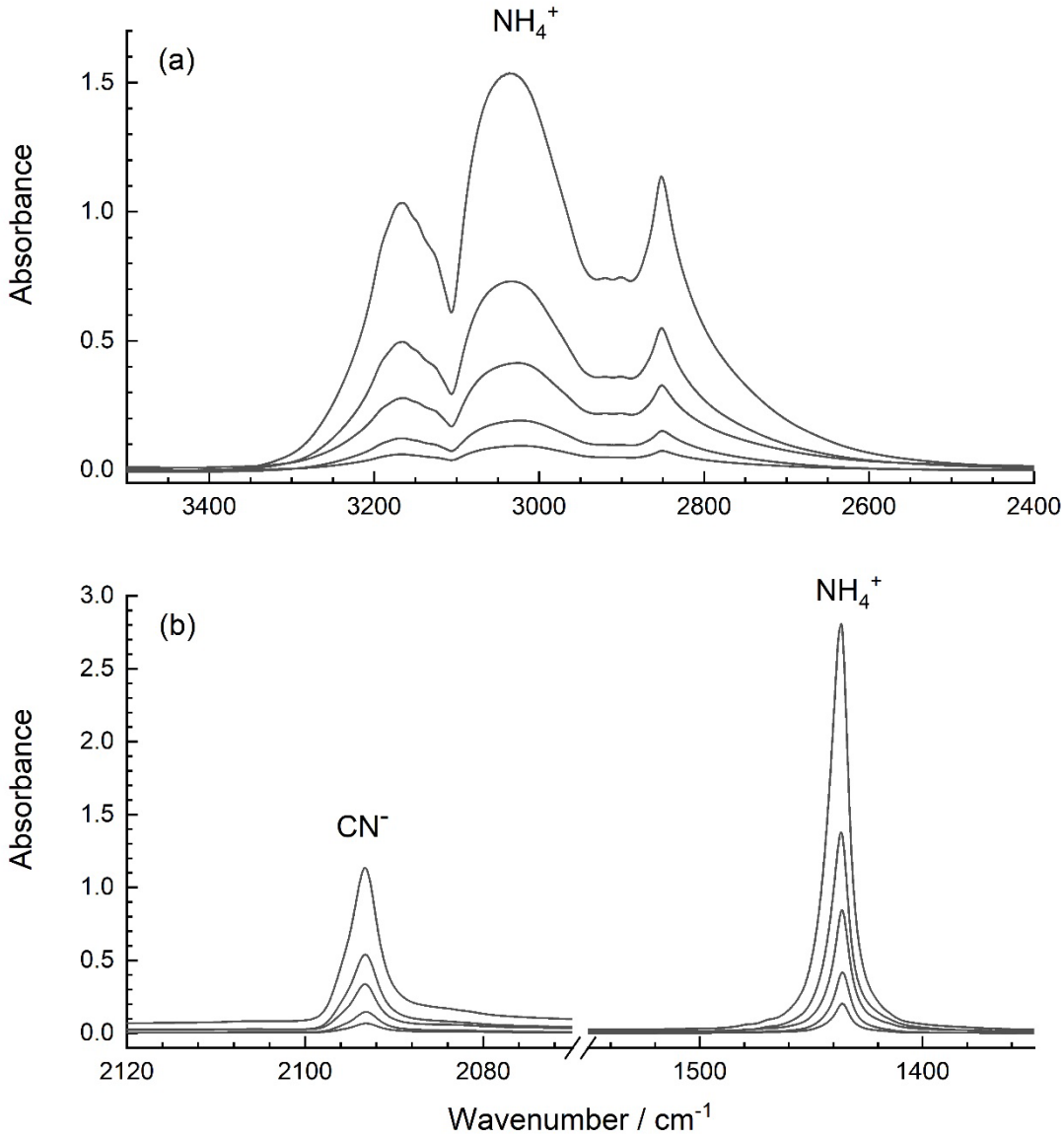

Fig. 3. Infrared spectra of five NH_4CN samples grown at 125 K to thicknesses of 0.11, 0.22, 0.43, 0.86, and 1.73 μm. Spectra have been separated and expanded to highlight the absorption features of (a) the N-H stretching bands of NH_4^+ and (b) the CN^- stretching and NH_4^+ deformation modes.

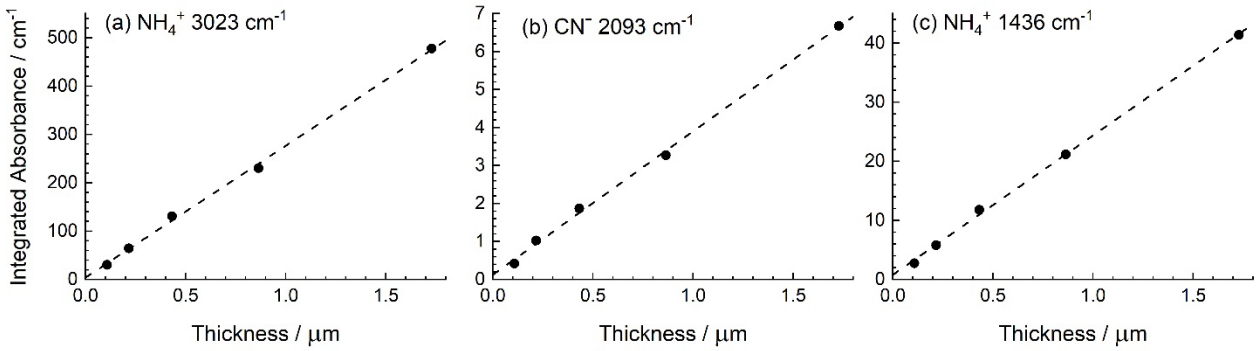

Fig. 4. Integrated absorbance vs. thickness for five NH_4CN samples created at 125 K. Panel (a) contains data for the 3023 cm^{-1} band of NH_4^+, (b) for the 2093 cm^{-1} band of CN^-, and (c) for the 1436 cm^{-1} band of NH_4^+. The linear least-squares best fit (R^2 > 0.996) is given by the dashed line in each case. Slopes of the fits and their uncertainties were used to derive the band strengths and uncertainties reported in Table 1 (see text for details).

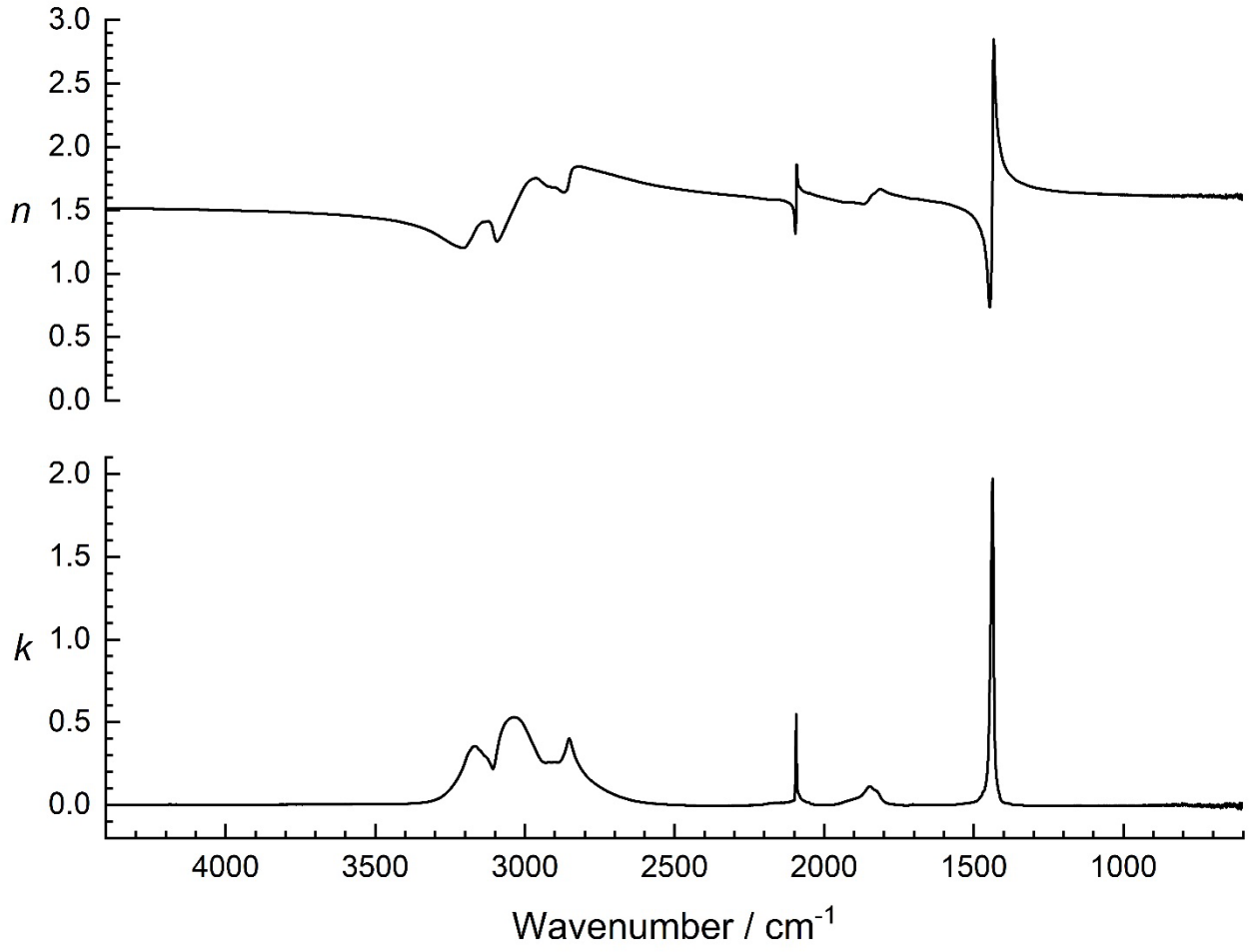

Fig. 5. Optical constants (*n* and *k*) for NH_4CN at 125 K from 4400 to 600 cm^{-1}.

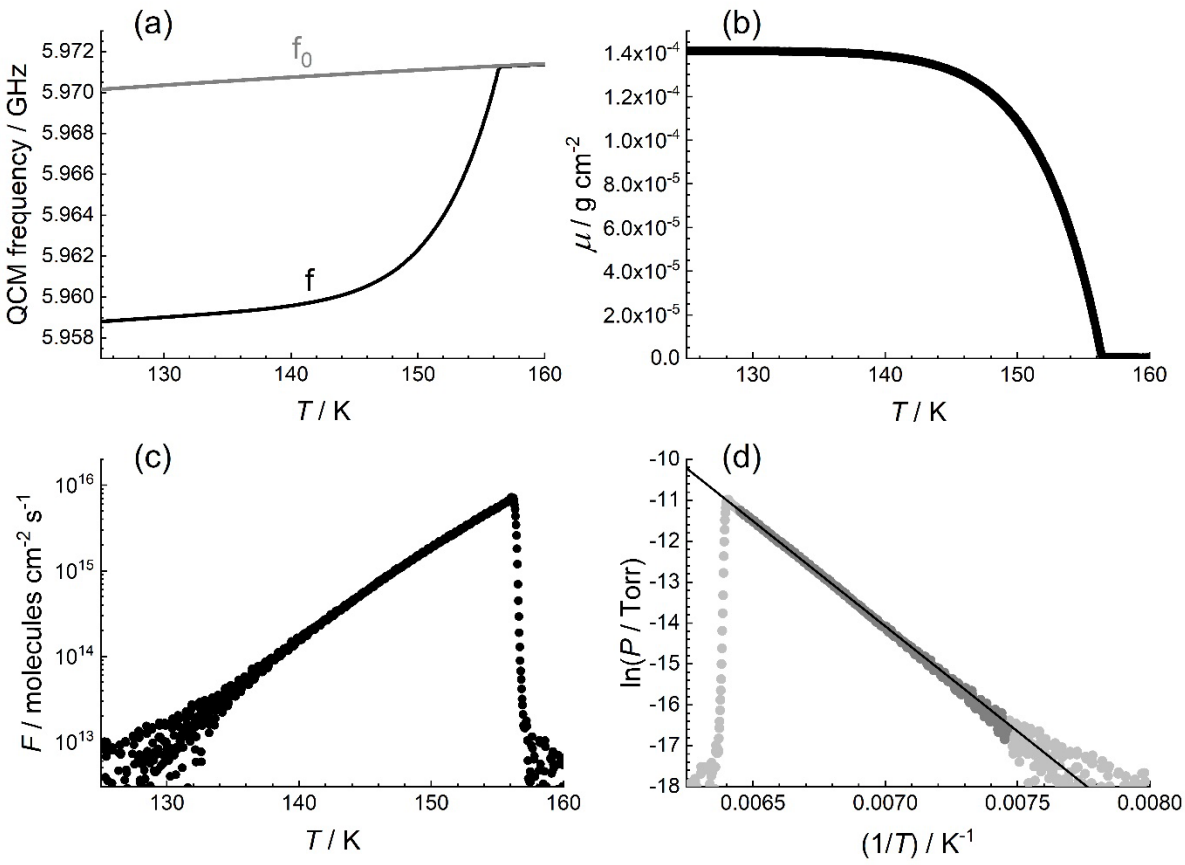

Fig. 6. Sublimation data from one of the NH_4CN samples. In panel (a), the measured QCM frequencies with a sample (black trace, f) and without a sample (gray trace, f_0) are plotted against temperature T during warm-up of the sample. In (b) and (c), the derived mass per unit area μ and sublimation flux F are plotted vs. T. Panel (d) shows the derived dissociation pressures in a plot of ln(P) vs. 1/T, where the line is the linear least-squares fit to the dark gray points from 134 to 155 K (0.00746 to 0.00645 K^{-1}). See text for details.

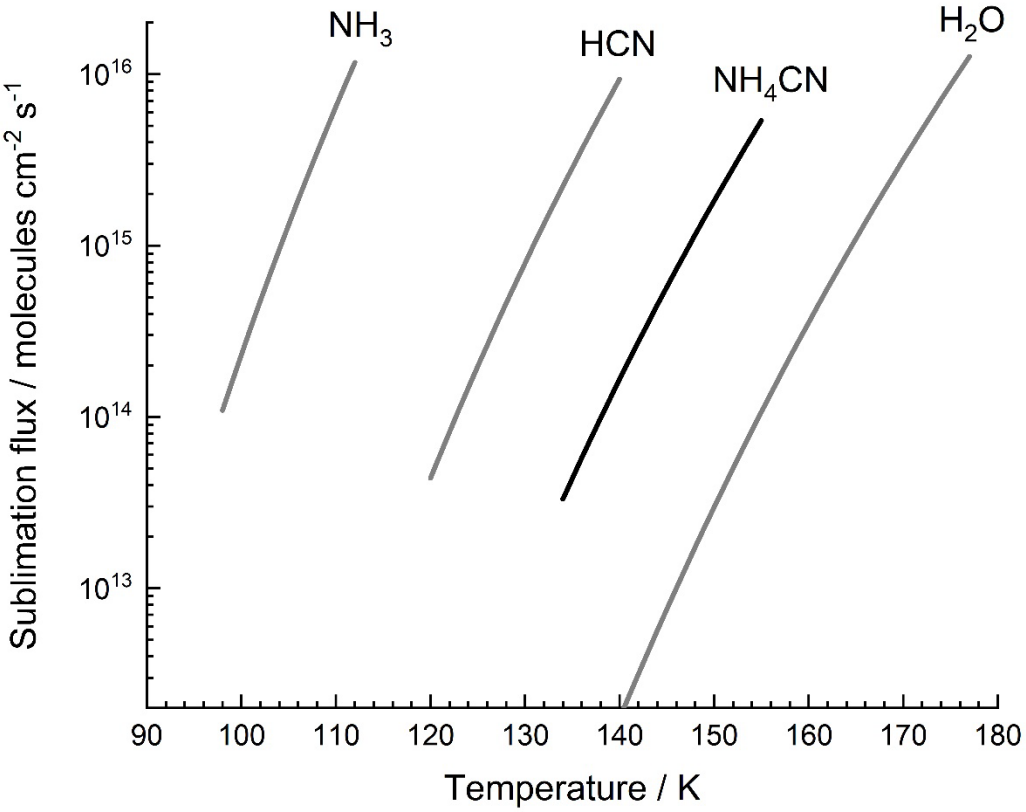

Fig. 7. Sublimation flux for NH_4CN (black curve) as given by the fit to our measurements and plotted over the fitted temperature range. Also shown are the corresponding curves for NH_3 from this work, HCN from Hudson and Gerakines (2023), and H_2O from Hudson et al. (2022b).

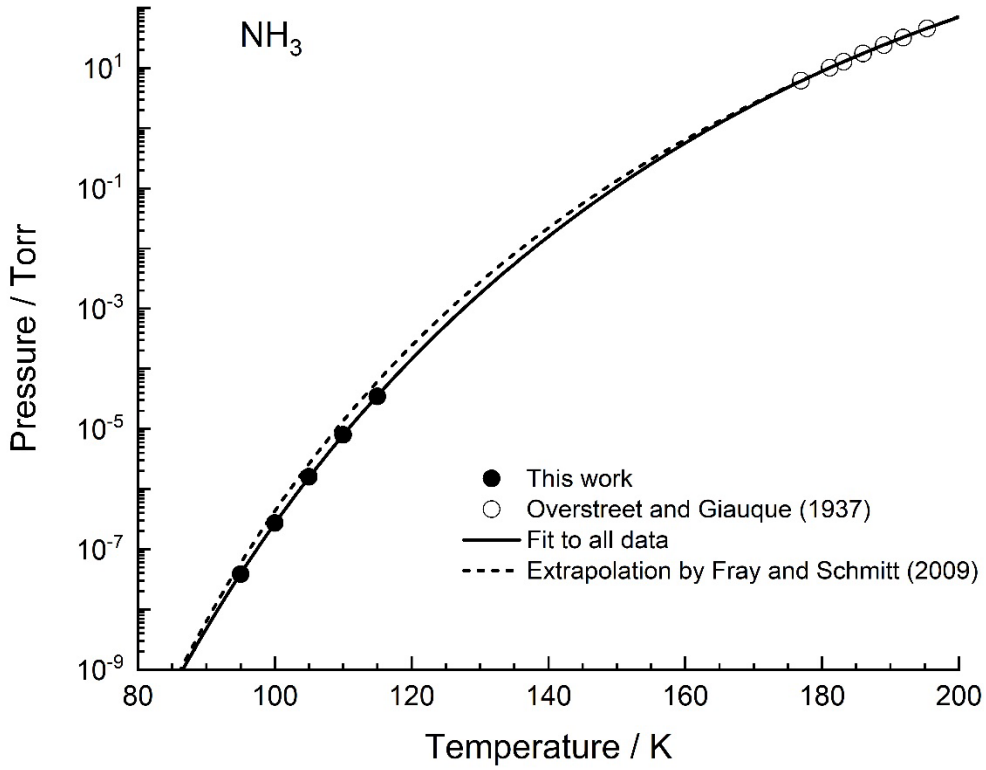

Fig. 8. Comparison of our measured NH_3 vapor pressures with data from other authors. Filled circles: values from Table 3. Empty circles: data from Overstreet and Giauque (1937). Solid curve: fit to all data points using the Cox equation (see text). Dashed curve: extrapolation to low temperatures suggested by Fray and Schmitt (2009).

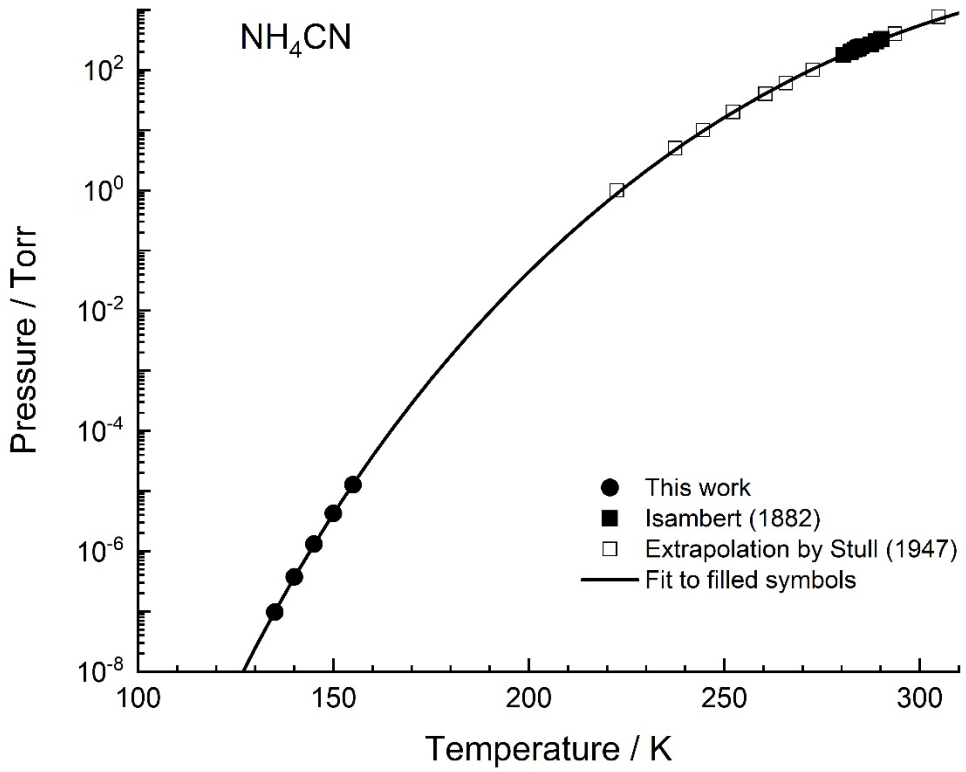

Fig. 9. Comparison of our measured NH_4CN vapor pressures with those from Isambert (1882). Filled circles: values from Table 3. Filled squares: values measured by Isambert (1882). Empty squares: extrapolated values listed by Stull (1947). Curve: fit to the filled symbols using the Cox equation (see text).